

Fig. 2—Setup stand for ultrasonic shear transducer

Experimental Techniques and the Determination of the Acoustoelastic Coefficient

The sing-around equipment used in the present experiments is shown in the block diagram Fig. 1. A 6-mm square, 0.2-mm thickness barium-titanate ceramic plate was used as a transmitting transducer of 5-MHz ultrasonic shear waves and a 4-mm square, 0.2-mm-thickness plate of the same material was used as a receiving transducer. Use of a smaller transducer as a receiver made it possible to catch the main part of the almost plane wavefront resulting in a sharp rising signal for the sing-around trigger. To reinforce the transducer mechanically and to reduce reflections of the wave at the end surface, an epoxy resin mixed with copper powder was cemented to the back surface of the transducer. The transducer was attached to the specimen by Canada balsam diluted with castor oil and, at the same time, it was pressed against the specimen by a spiral spring installed in a setup stand, which is shown in Fig. 2. In this way, the system transmits high-frequency shear waves into specimen quite efficiently. The transducer is rotatable without demounting it from the specimen during the test by loosening the spring pressure.

To determine the basic acoustoelastic coefficient of the mild steel, uniaxial tests were carried out on specimens of size 60 mm \times 60 mm \times 20 mm made from the same material. We depended exclusively on compression tests because, as was shown in a previous paper,³ the acoustoelastic coefficients in this material coincided both for tension and compression tests. Axial directions of the specimen were parallel or perpendicular to the rolling direction of the original material. The specimen surfaces on which the transducer was attached were well ground. A 30-ton universal testing machine was used to load the specimen. As the sing-around measurement of a transit time was very sensitive to environmental temperature, the region of the specimen and the sing-around instrument was enclosed by partition walls made by foaming polystyrol plates and ventilated by two fans to keep temperature as constant as possible.

The transducer was first polarized in the loading direction and the transit time of the shear wave across the specimen under stress was measured at preselected

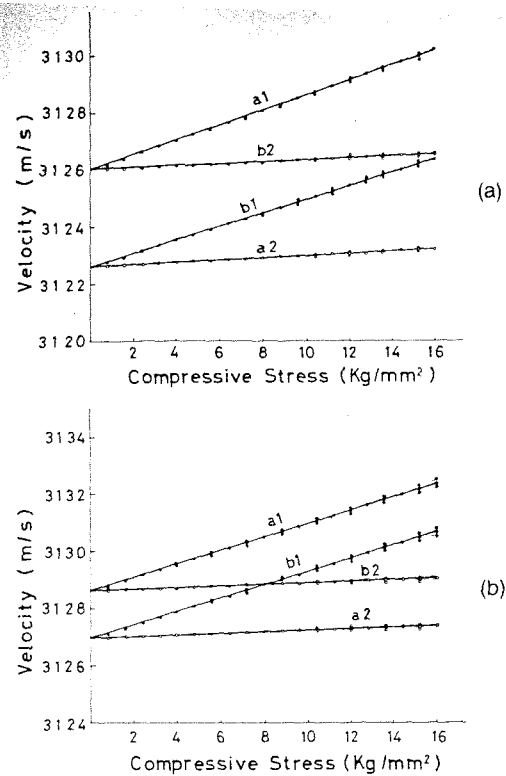


Fig. 3—Stress-velocity relation for mild steel. (a) As-rolled material; (b) tempered material. Notation: a—loading direction is parallel to rolling direction; b—loading direction is perpendicular to rolling direction. 1—polarization is parallel to loading direction; 2—polarization is perpendicular to loading direction

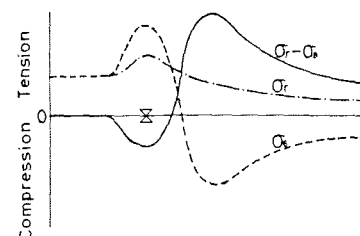
levels for both loading and unloading. Then the transducer was rotated so that the direction of polarization was perpendicular to the loading direction and measurements of the transit time were carried out similarly. The measurements were done three times for each load level. In the present experiments, the delay time for a pulse in the circuit was 128 μ s and the sing-around repetition was 10,000. The transit time was measured by an electronic counter having a reference frequency of 10 MHz. The sensitivity of the sing-around measurement was 10 picoseconds in transit time. When the environmental temperature was kept within $\pm 0.1^\circ\text{C}$, the variation of the counter reading was about 30 picoseconds during the test. After tests had been done for three specimens in the as-rolled state, these specimens were tempered at 900°C for one hour and subsequently air cooled. Then the measurements of the stress-induced velocity changes were repeated.

The test results are shown in Fig. 3 in the form of a stress-velocity relation. Discrepancies of velocities for waves polarized parallel and perpendicular to loading directions

TABLE 1—ACOUSTOELASTIC COEFFICIENTS OF MILD STEEL USED IN THE PRESENT EXPERIMENTS. UNITS ARE IN $(\text{kg}/\text{cm}^2)/(\text{cm}/\text{s})$.

	As-rolled	Tempered
Loading direction is parallel to rolling direction	4.5×10^{-2} $\pm 0.25 \times 10^{-2}$	4.8×10^{-2} $\pm 0.30 \times 10^{-2}$
Loading direction is perpendicular to rolling direction	5.1×10^{-2} $\pm 0.35 \times 10^{-2}$	5.0×10^{-2} $\pm 0.35 \times 10^{-2}$
Average	4.8×10^{-2}	4.9×10^{-2}

Fig. 4—Theoretical prediction for residual-stress distribution in patch-welded circular plate Σ indicates position of welding line



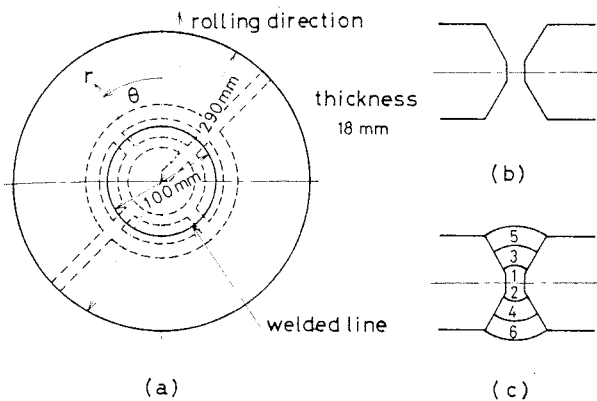


Fig. 5—(a) Patch-welded disk specimen. Dotted line indicates sectioning for destructive strain-gage measurement of residual stress. (b) Edge preparation. (c) Deposited sequences

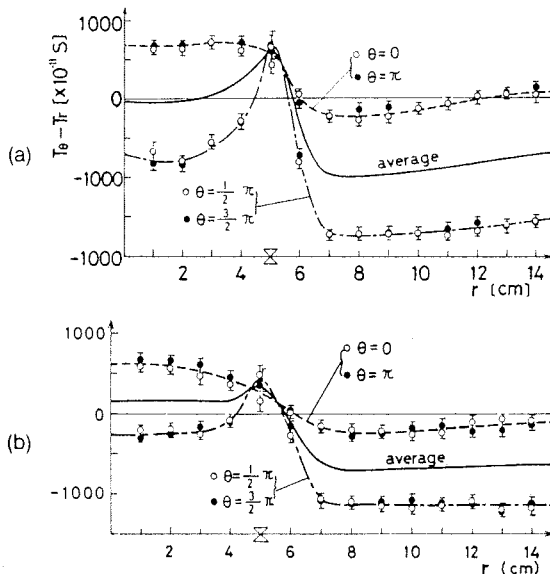
for each specimen at zero stress level indicate anisotropy due to a preferred orientation. All the measurements show substantially linear stress-velocity relations. Therefore the acoustoelastic coefficients are obtained from the slopes of stress-velocity difference lines as are shown in Table 1.

It must be emphasized here that the present method gives only the information of the stress state averaged through the thickness of the specimen.

Measurement of Residual Stress in a Patch-welded Circular Plate

Based on the notion of inherent strain uniformly distributed along the circumferential welding line, residual-stress distributions in a finite circular plate with concentrically patch-welded joints were calculated⁷ with the results shown in Fig. 4, which agreed quite well with experimental results obtained by a destructive sectioning procedure. A typical nondestructive method of residual-stress measurement is that of X-ray diffraction, in which stresses are evaluated by measuring the changes in lattice spacing. Because the X-rays penetrate less than 0.02 mm into the surface of a metal, this method is limited to a measurement of surface stresses only.

Fig. 6—Difference of transit time for two kinds of shear waves. (a) Disk made from as-rolled material. (b) Disk made from tempered material



We thus apply the acoustoelastic stress analysis to measure residual stresses in the patch-welded circular plate. The test specimen is shown in Fig. 5(a). The preparation of the specimen and the weld-deposition sequences are shown in Fig. 5(b) and 5(c). The welded-bead part was finished by a plane-grinding machine. Two specimens were tested: one was made from as-rolled plate and the other from the plate tempered at 900°C for one hour and subsequently air-cooled. We chose the rolling direction of the original material as $\theta = 0$ [Fig. 5(a)]. The measurement for the stress-induced velocity changes was carried out for 14 points along radial directions of $\theta = 0, \pi/2, \pi$ and $(3/2)\pi$.

As we assumed the principal directions of residual stress to be radial and circumferential, the transit time of shear waves polarized in radial and circumferential directions was measured by the sing-around method in the same way as for the compression tests to determine the acoustoelastic coefficient.

The results of these measurements are shown in Fig. 6, in which the abscissa represents radial position from the center of the disk and the ordinate indicates the differences of transit time between the waves polarized in radial and circumferential directions. Measurements were carried out several times for each point.

As the residual-stress distribution was assumed to be axisymmetric, discrepancies in data obtained from $\theta = 0$ and π and from $\theta = \pi/2$ and $(3/2)\pi$ should be attributed to anisotropy due to preferred orientation. As is seen from Fig. 6, the original preferred orientation due to rolling, which does not depend on the radial distance, is reduced considerably near the welding line having been exposed to temperatures close to the melting point of the material. Averaging the data of the same radial distance from the center of the disk, we thus obtain the values of propagation velocities independent of the effects of a preferred orientation.

Figures 7(a) and (b) show the residual-stress distributions of the patch-welded circular plate, obtained from the data in Fig. 6, by making use of the acoustoelastic coefficient of this material. The acoustical measurements are denoted with I-marks, and the values obtained from the conventional destructive method are denoted by solid and hollow circles. The latter were obtained from strain-gage measurements before and after the disk was sectioned into pieces, as shown in Fig. 5(a), with the dotted lines. It is shown that the results obtained by acoustoelasticity agree well with those obtained by the conventional destructive method, as well as the theoretical prediction shown in Fig. 4. It is also shown that residual stresses in the disk made from as-rolled material are larger than those in the disk made from the tempered material.

Conclusions

The technique of acoustoelastic stress analysis employed in this paper uses the velocity difference in ultrasonic shear waves polarized in principal directions by means of the sing-around method. To illustrate the applicability of this technique to nondestructive stress analysis, the residual-stress distribution in a patch-welded circular plate was measured. It was found that the results obtained by the acoustoelastic method agreed well with those obtained by the conventional destructive method.

We conclude that the acoustoelastic stress analysis seems to be one of the most promising techniques for non-destructive stress analysis, although there are still many difficult problems to overcome, notably those of transducer-coupling materials and separation of preferred

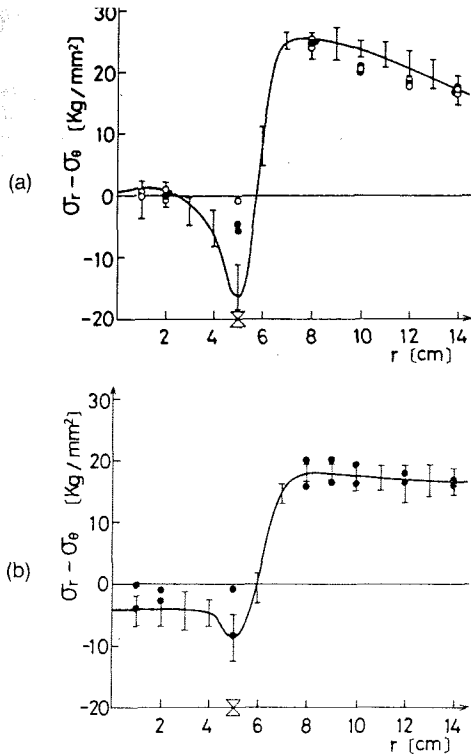


Fig. 7—Residual-stress distribution.
 (a) Disk made from as-rolled material.
 (b) Disk made from tempered material.
 I-mark: acoustoelasticity measurement.
 Circles: destructive strain-gage measurement. Hollow circle in (a) indicates data from the gage attached on the reverse side of the disk

orientation effects.

Acknowledgments

The authors wish to thank K. Yaegawa, F. Natsumi and K. Mori for their assistance. Thanks are also due to Y. Ueda of Welding Research Institute of Osaka University for his advice to prepare the patch-welded circular plate and discussions on residual stresses in the welded structure. Finally, they would like to express their gratitude to the reviewers for their comments and advice which have led to the improvement of the original manuscript.

References

1. Crecraft, D.I., "The Measurement of Applied and Residual Stresses in Metals Using Ultrasonic Waves," *J. Sound Vib.*, 5, 173-192 (1967).
2. Hsu, N.N., "Acoustic Birefringence and the Use of Ultrasonic Waves for Experimental Stress Analysis," *EXPERIMENTAL MECHANICS*, 14 (5), 169-176 (May 1974).
3. Fukuoka, H. and Toda, H., "Preliminary Experiment on Acoustoelasticity for Stress Analysis," *Archives of Mechanics*, 29 (5), 673-686 (1977).
4. Blinka, J. and Sachse, W., "Application of Ultrasonic-pulse-spectroscopy Measurements to Experimental Stress Analysis," *EXPERIMENTAL MECHANICS*, 16 (12), 448-453 (Dec. 1976).
5. Tokuoka, T. and Iwashimizu, Y., "Acoustical Birefringence of Ultrasonic Waves in Deformed Isotropic Elastic Materials," *Int. J. Solids Struct.*, 4, 338-389 (1968).
6. Tokuoka, T. and Iwashimizu, Y., "Acoustoelasticity," *Science of Machine (in Japanese)*, 27, 860-864 (1975).
7. Fujimoto, T., "Residual Stresses in Patch Welded Circular Plates," *J. Japan Weld. Soc. (in Japanese)*, 43, 119-126 (1974).

ERRATA:

Experimentally Determined Stress-intensity Factors for Single-edge-crack Round Bars Loaded in Bending

by Arthur J. Bush

On pages 249-257 of the July 1976 issue of *EXPERIMENTAL MECHANICS*, there appeared the paper "Experimentally Determined Stress-intensity Factors for Single-edge-crack Round Bars Loaded in Bending" by Arthur J. Bush.

Due to the unfortunate "splicing" of the wrong negatives by the printer, immediately before going to press (that is, after the correctly prepared page proofs had been approved and released for printing by the editors), the data given in Table 4 were repeated in Table 2, and the information intended for Table 2 was never used.

The correct Table 2 is reproduced at right.

The error was brought to our attention by the author in August 1977. He is in no way responsible for the long, although unavoidable, delay in the publication of this correction.

The Editors

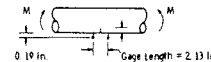
TABLE 2—COMPLIANCE AND CRACK-OPENING-DISPLACEMENT DATA FOR 3-in. (76-mm) HOLLOW SEC-RBB SPECIMENS 3-3 AND 3-6

Crack ⁽¹⁾ Length	a/D	Compliance ⁽²⁾⁽⁵⁾	COD ⁽³⁾
a		c	
(in.)		(10 ⁻⁶ in./lb.)	(10 ⁻⁶ in./lb.)
Specimen 3-3 ⁽⁴⁾			
0.0	0.0	4.195	0.438
0.100	0.033	4.316	0.449
0.202	0.067	4.440	0.472
0.400	0.133	4.535	0.551
0.653	0.218	5.679	0.742
0.851	0.284	6.096	0.999
0.949	0.316	6.342	1.193
1.001	0.334	6.769	1.325
1.045	0.348	1.905	1.466
1.198	0.399	7.897	1.962
1.397	0.466	9.485	2.807
1.594	0.531	12.537	4.277
Specimen 3-6 ⁽⁴⁾			
0.403	0.134	4.993	0.523
0.523	0.174	5.257	0.586
0.653	0.217	5.358	0.748
0.752	0.251	5.696	0.882
0.901	0.300	6.289	1.128

(1) Crack length is depth of machined notch.

(2) Compliance "c" is the inverse slope of the load-displacement curve, or "v/p".

(3) COD is the crack-opening-displacement as measured in routine fracture toughness tests. COD was measured 0.19 in. from the front face of the specimen as shown:



(4) Specimen 3-3 outer diameter was 3.006 in. and 3-6 was 3.001 in.; for both bars the inner diameter was 1.00 in.

(5) The min-max regression computer-fitted equation for $c = f(a/D)$ with $n = 2.5$ is:

$$c = b_0 + b_1 (a/D)^{2.5}$$

where $b_0 = 4.453971$ and $b_1 = 37.88840$

S1 Conversion: mm = in. x 25.4 and kN = lb. x 0.00445.